A Tectonic Origin for the Largest Marsquake Observed by InSight

Benjamin Fernando, Ingrid Daubar, Constantinos Charalambous, Peter Grindrod, Alexander Stott, Abdullah Al Ateqi, Dimitra Atri, Savas Ceylan, John Clinton, Matthew Fillingim, et al.

AGU ADVANCING EARTH AND SPACE SCIENCES

Geophysical Research Letters®

RESEARCH LETTER
10.1029/2023GL103619

Special Section:
The Large Marsquake of Sol 1222

A Tectonic Origin for the Largest Marsquake Observed by InSight

Benjamin Fernando[1], Ingrid J. Daubar[2], Constantinos Charalambous[3], Peter M. Grindrod[4], Alexander Stott[5], Abdullah Al Ateqi[6], Dimitra Atri[6], Savas Ceylan[7], John Clinton[7], Matthew Fillingim[8], Ernest Hauber[9], Jonathon R. Hill[10], Taichi Kawamura[11], Jianjun Liu[12], Antoine Lucas[11], Ralph Lorenz[13], Lujendra Ojha[14], Clement Perrin[15], Sylvain Piqueux[16], Simon Stähler[7], Daniela Tirsch[9], Colin Wilson[17], Natalia Wójcicka[18], Domenico Giardini[7], Philippe Lognonné[11], and W. Bruce Banerdt[16]

[1]Department of Physics, University of Oxford, Oxford, UK, [2]Department of Earth, Environmental, and Planetary Sciences, Brown University, Providence, RI, USA, [3]Department of Electrical and Electronic Engineering, Imperial College London, London, UK, [4]Natural History Museum, London, UK, [5]ISAE-SUPAERO, Toulouse, France, [6]Center for Space Science, New York University, Abu Dhabi, UAE, [7]Department of Earth Sciences, ETH Zurich, Zurich, Switzerland, [8]Space Sciences Laboratory, University of California Berkeley, Berkeley, CA, USA, [9]Institute of Planetary Research, German Aerospace Center (DLR), Berlin, Germany, [10]School of Earth and Space Exploration, Arizona State Univeristy, Tempe, AZ, USA, [11]Institut de Physique du Globe de Paris, CNRS, Université Paris Cité, Paris, France, [12]National Astronomical Observatories, Chinese Academy of Sciences, Beijing, China, [13]Applied Physics Laboratory, Johns Hopkins University, Baltimore, MD, USA, [14]Department of Earth and Planetary Sciences, Rutgers University, New York, NY, USA, [15]Laboratoire de Planétologie et Géosciences, Nantes Université, Nantes, France, [16]Jet Propulsion Laboratory, California Institute of Technology, Pasadena, CA, USA, [17]European Space Agency, Noordwijk, The Netherlands, [18]Department of Earth Science and Engineering, Imperial College London, London, UK

Key Points:

- The S1222a marsquake detected by InSight on 4 May 2022 somewhat resembled previous impact-generated events
- We performed an image search in the estimated source region, using data from multiple Mars orbiter missions
- No new impact crater has been discovered in this area, pointing to a tectonic origin for the quake

Supporting Information:

Supporting Information may be found in the online version of this article.

Correspondence to:

B. Fernando,
benjamin.fernando@physics.ox.ac.uk

Citation:

Fernando, B., Daubar, I. J., Charalambous, C., Grindrod, P. M., Stott, A., Al Ateqi, A., et al. (2023). A tectonic origin for the largest marsquake observed by InSight. *Geophysical Research Letters*, *50*, e2023GL103619. https://doi.org/10.1029/2023GL103619

Received 14 MAR 2023
Accepted 15 SEP 2023

Abstract The S1222a marsquake detected by InSight on 4 May 2022 was the largest of the mission, at M_w^{Ma} 4.7. Given its resemblance to two other large seismic events (S1000a and S1094b), which were associated with the formation of fresh craters, we undertook a search for a fresh crater associated with S1222a. Such a crater would be expected to be ~300 m in diameter and have a blast zone on the order of 180 km across. Orbital images were targeted and searched as part of an international, multi-mission effort. Comprehensive analysis of the area using low- and medium-resolution images reveals no relevant transient atmospheric phenomena and no fresh blast zone. High-resolution coverage of the epicentral area from most spacecraft are more limited, but no fresh crater or other evidence of a new impact have been identified in those images either. We thus conclude that the S1222a event was highly likely of tectonic origin.

Plain Language Summary During its time on Mars, NASA's InSight (Interior Exploration using Seismic Investigations, Geodesy and Heat Transport) mission recorded over 1,300 seismic events, known as "marsquakes." Of these, a number were identified as coming from meteoroid impact cratering events on the surface. The largest event identified by InSight, labeled S1222a, bore some similarities to two large impact events recorded earlier in the mission. In order to investigate whether the S1222a event might also have been caused by an impact event, we undertook a comprehensive search of the region in which the marsquake occurred. We did not identify any fresh craters in the area, implying that the marsquake was likely caused by geological processes.

1. Introduction

On 4 May 2022, NASA's InSight mission recorded the seismic waves from an event on Mars of magnitude M_w^{Ma} 4.7 ± 0.2. This event, labeled S1222a in the catalog, was the largest of the mission and displayed characteristics spanning all previously identified marsquake families (Ceylan et al., 2022). It also displayed clear evidence of surface waves (Kawamura et al., 2022).

Seismic data were recorded on the InSight's Very Broad Band Seismometer (Banerdt et al., 2020; Lognonné et al., 2019). Based upon travel time differentials and signal polarization, this event was located within a near-ellipse with an epicenter near 3.0°S, 171.9°E; 37° or ~2200 km from InSight (see Kawamura et al. for more details including contextual map). This region is just north of the dichotomy boundary. Orbital images indicate the presence of wrinkle ridges in the region, which could indicate past tectonic activity nearby. Otherwise, the

region is largely flat and thermal inertia indicates a predominantly dusty surface, conducive to the detection of a fresh crater from orbital images if one exists (Lucas et al., 2023) find evidence of enhanced avalanche rates in the area, potentially indicative of surface-wave induced shaking but at a far smaller scale than would be required to excite the event itself.

Surface waves had only been identified previously for two other events, both in 2021: S1000a (126.7° away) and S1094b (58.5° away) (Kim et al., 2022), at magnitudes M_w^{Ma} 4.1 ± 0.2 and M_w^{Ma} 4.0 ± 0.2, respectively (Ceylan et al., 2022). In the case of both S1000a and S1094b, orbital image searches confirmed the presence of large, fresh craters at the expected seismic epicenters. The formation times of these craters matched the occurrence times of the events, indicating that they were of meteoroid impact origin (Posiolova et al., 2022). Both craters were in the 100–200 m diameter range, significantly larger than both the average size of new martian craters in the present era (Daubar et al., 2022) and the other impact events detected seismically by InSight (Daubar et al., 2023; Garcia et al., 2022).

Owing to their frequency content, all three events, S1222a, S1094b, and S1000a have been classified as broadband by the MarsQuake Service (MQS) (Ceylan et al., 2022; Kawamura et al., 2022). Figure 1 shows filtered time-domain seismograms of S1222a compared to the two confirmed impacts, arranged by increasing epicentral distance. The signal is shown filtered into two main frequency bands of 0.05–1 Hz and 1–8 Hz, in order to demonstrate both the comparative low-frequency and high-frequency content of the three events. These bands are chosen as they are close to those used by MQS to classify events on Mars (InSight Marsquake Service, 2023). Spectrograms of these events are also shown in Figure 2. Due to the power constraints faced by the InSight lander during this time, all atmospheric sensors were off at the time of S1222a and hence neither pressure nor wind data exist.

There are numerous similarities between S1222a and the two confirmed impact events. All three events show:

- Long-period surface wave trains; these are also the only three events with identified surface waves.
- Energy spanning a broad range of frequencies, across a broader spectrum than most other events.
- Long-duration codas, with low-frequency energy (<1 Hz, lasting up to ∼10.5 hr for the larger S1222a event and 1.5–2 hr for both S1000a and S1094b (InSight Marsquake Service, 2023)).

However, some differences are also apparent in addition to the much larger magnitude of S1222a:

- S1222a includes a significantly richer family of surface-wave arrivals, including not only fundamental Rayleigh waves (R1) but also Love waves (G1).
- S1222a also displays overtones and successive multi-orbit major- and minor-arc Rayleigh waves, unlike the two large impact events.
- The S1222a ratio of P-wave energy to S-wave energy is lower than for S1000a or S1094b in the highest frequency bands (Figure 1b). This may indicate a greater deviatoric component to the source mechanism (Taylor et al., 2002; Walter et al., 2018) as may occur from a double-couple fault rather than an isotropic explosive impact source.

Given the extraordinary nature of the S1222a event, and the above similarities to the large confirmed impacts of S1000a and S1094b, it was prudent to consider the possibility of an impact origin. Thus an effort was mounted to search for a fresh crater or other transient signal (e.g., an impact-generated dust cloud) associated with this event that would prove an impact origin.

If S1222a were an impact event, the crater size would likely have been extremely large (≥300 m). This estimate is based upon the relationship between seismic moment and crater diameter; where the seismic moment is expected to scale with crater diameter to the power of ∼3.3. This estimate is informed by impact modeling results and calibrated against a set of small seismically detected impacts on Mars (Wojcicka et al., 2020; Wójcicka et al., 2023). The expected recurrence interval for a crater of this size across the entirety of Mars is on the order of ∼100 years (Hartmann & Daubar, 2017).

It should be noted that the size of this event means that the scaling relationship is extrapolated significantly, and hence the predicted diameter estimate for S1222a comes with broad uncertainties. Similarly speculative extrapolation of observed relationships between smaller new impacts and their halos (Bart et al., 2019) suggests that such a crater would have a blast zone (an area where dust has been removed by the atmospheric effects of the meteoroid entry and/or impact, causing a surficial albedo change) in the ∼180 km diameter range.

The S1000a and S1094b craters produced blast zones large enough to be visible in low-resolution images from MRO's Mars Color Imager (MARCI) (Bell et al., 2009; Posiolova et al., 2022). Under similar surface conditions an impact event of this size would also have been expected to produce a large blast zone.

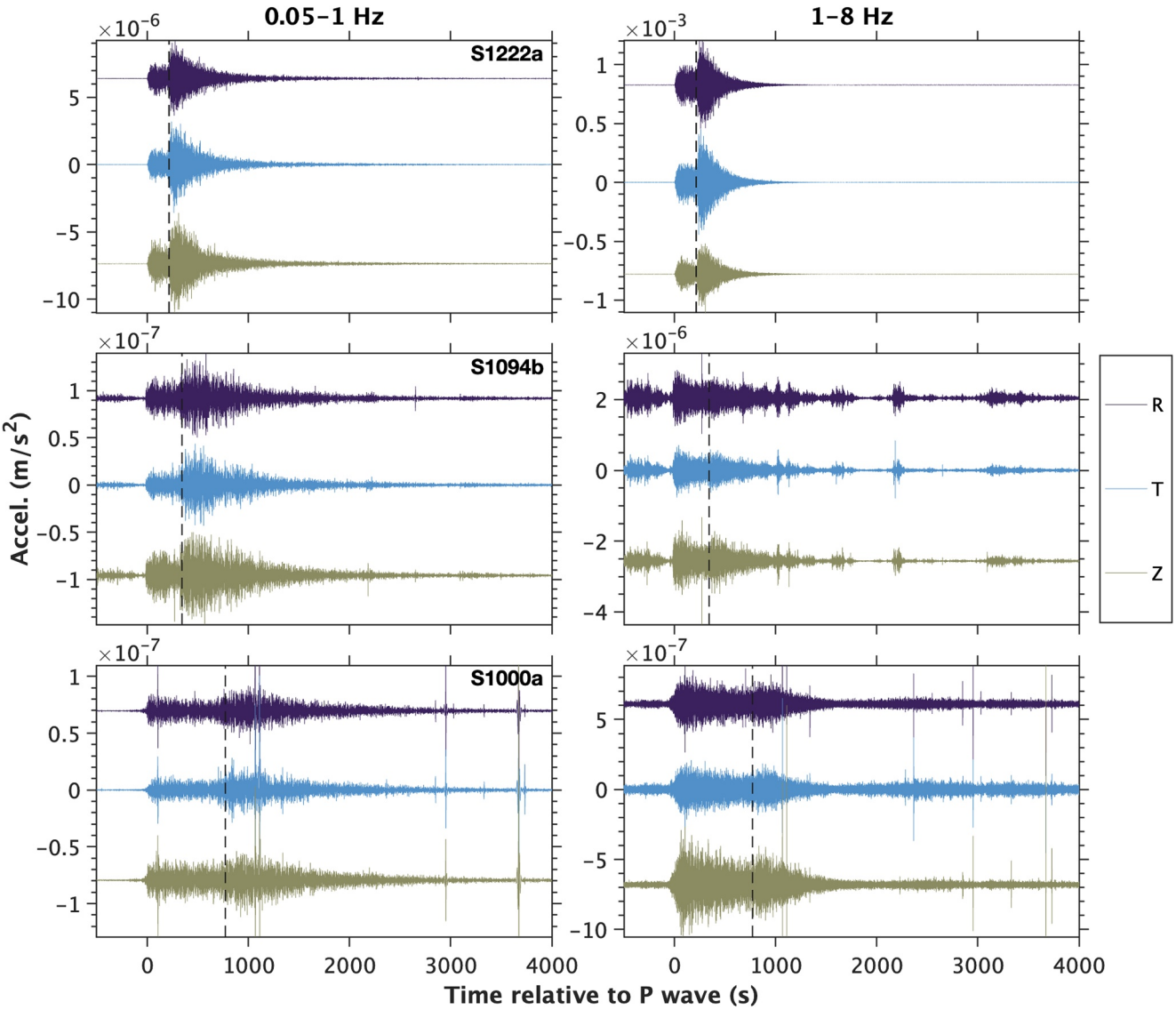

Figure 1. Seismograms from the S1222a event and the two confirmed impact-generated events, S1000a and S1094b. Acceleration data are presented from InSight's Very Broad Band sensor. Two frequency bands are shown: 0.05–1 Hz (left) and 1–8 Hz (right). The waveforms have been rotated to radial, transverse and vertical (RTZ) directions using the estimated back azimuth information (for S1222a) (Kawamura et al., 2022) and the measured back azimuth from imaged crater locations (for S1094b and S1000a) (Posiolova et al., 2022). Seismograms are aligned at zero seconds by the first P-wave arrival (PP for S1000a), while the dashed lines indicate the first S-wave arrival (SS for S1000a) (Ceylan et al., 2022).

Conversely, a lack of a fresh crater or blast zone, given surface images of sufficient coverage and resolution, would be a strong indication of a non-impact/tectonic origin. This paper describes that search, excluding the formation of smaller or more irregular crater(s) due to atmospheric breakup or impact into steep topography.

This paper constitutes an international collaboration between all of the missions currently operating in orbit at Mars. We hope that it will also prove a useful template for similar collaborations in the future.

2. Methodology

2.1. Crater-Seismic Associations

Making the association between a given seismic event and a fresh crater is challenging. This is partly due to the limited number of camera-equipped spacecraft in orbit around the planet. They make infrequent overpasses of any given area, and come with limitations on data volume and operational constraints on imaging. It is also partly due

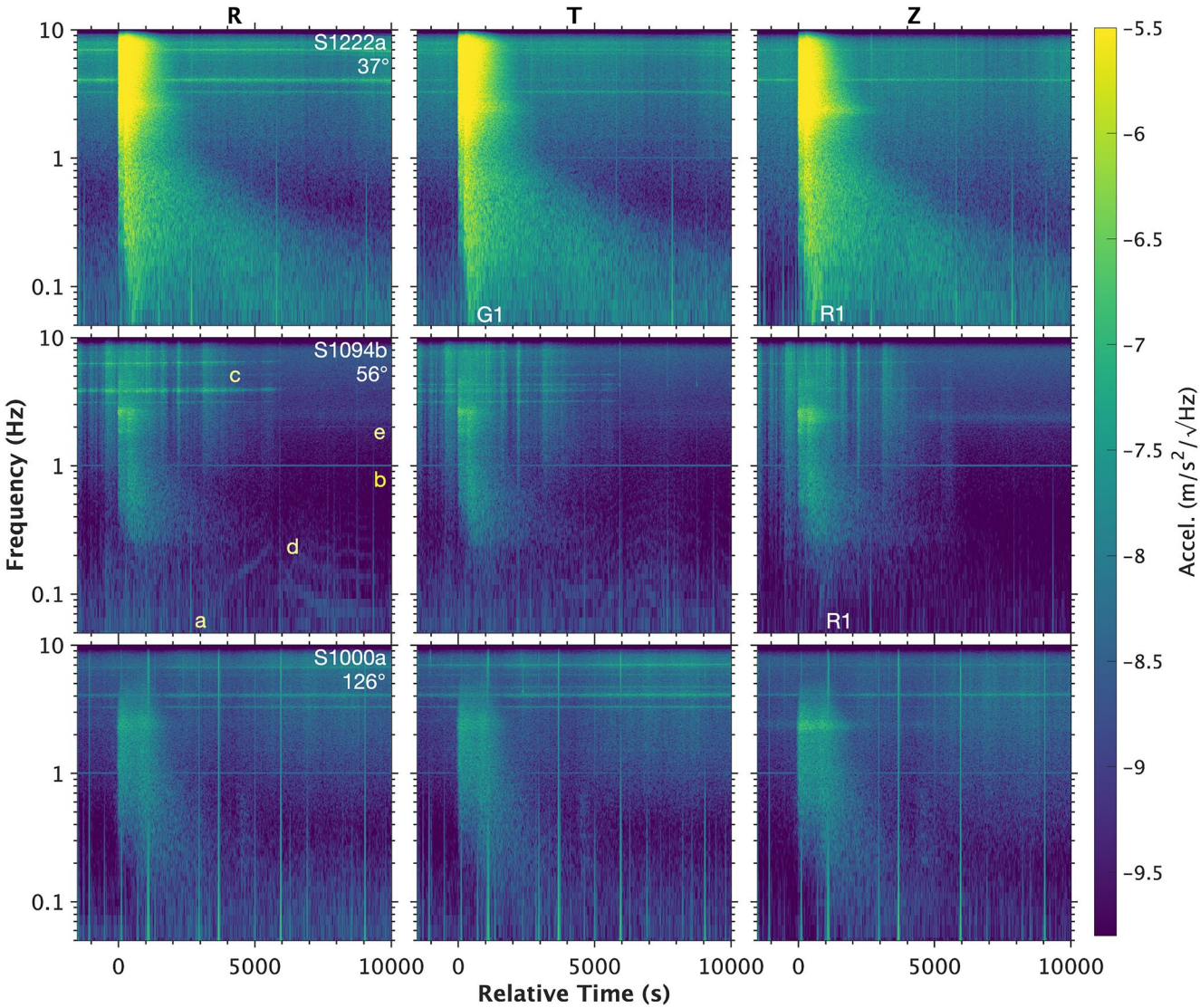

Figure 2. Acceleration spectrograms of the S1222a, S1094b, and S1000a events rotated into the source-centered coordinate system (RTZ), as in Figure 1. The spectrograms are calculated using 80 s long Hanning windows of the continuous 20 samples/s Very Broad Band acceleration. Time is relative to P-wave arrival (PP for S1000a). *Signal*: Surface waves have been observed for all three events; fundamental Love waves (G1) and Rayleigh waves (R1) can be viewed by the naked eye for frequencies below 0.15 Hz at ~360 s in the T component and ~500 s in both R and Z components for S1222a (Kawamura et al., 2022), while the R1 for S1094b arrives ~800 s later and is visible in the Z component (Kim et al., 2022). *Noise*: several noise sources are apparent in all spectrograms: (a) high-amplitude transient spikes which are glitches or donks; (b) the persistent horizontal feature at 1 Hz is tick noise (Ceylan et al., 2021). (c) Broadband noise and lander resonances can be seen co-excited by atmospheric injection during windy periods (Charalambous et al., 2021), with the modes appearing as horizontal features at several frequency bands, with the most prominent at 4 Hz. (d) Dispersive patterns with overtones emerging during the latter half of S1094b correspond to sunset chirps, a daily feature in late afternoon most visible after the windy period ends (Ceylan et al., 2021). (e) The 2.4 Hz resonance is observed consistently during the quiet evening period and excited by all three events.

to the fact that most fresh craters of interest are sub-pixel size in images taken with all but the highest-resolution instruments. Complex surface topography, for example, steep slopes, can also further complicate matters by disguising fresh craters to the point that they are difficult to recognize from orbit (Daubar et al., 2023).

2.2. Blast Zone Detection

In dusty areas, fresh craters are surrounded by blast zones (regions where the shockwave from the incoming meteoroid has interacted with the surface). These can be tens or even hundreds of times larger than the crater itself (Bart et al., 2019), and as such are often the first component of a fresh crater to be identified in orbital images.

As blast zones fade on the order of decades (Daubar et al., 2016), they can be used to indicate geologically recent impact phenomena.

Although the larger areal extent of fresh blast zones as compared to fresh craters generally simplifies the search problem, the exact surface conditions and processes involved in their formation remain unclear (Daubar et al., 2013, 2022). Blast zones are more prevalent on dusty surfaces (and the S1222a search area is indeed dusty), but they can also be obscured or disguised by local heterogeneities or topography.

Thus, whilst low-resolution image searches could be sufficient to confirm an impact-generated hypothesis, alone they are not sufficient to exclude one in the case of a non-detection, as a blast zone might be missed. Searches for associated transient phenomena and high-resolution sampling of key areas must be used to reinforce our conclusion of a non-detection of a fresh crater of the requisite size.

2.3. Image Analysis

Images taken as part of our search campaigns can be divided into two categories: repeat images where visual change detection is possible, and those where fresh features are sought without past reference.

In the first category, where "before" images of a given region exist, post-event "after" images can also be captured to enable direct change detection. This is generally easier if the same instrument is used for both images in a before-after pair.

However, recent high-resolution coverage of Mars' surface is limited, meaning that in many places only suitable "after" images exist. In such cases, searches can only seek to identify fresh craters; which may be identified as "fresh" through features of their morphology, ejecta, and blast zones.

2.4. Potentially Observable Features

High-resolution instruments such as High-Resolution Imaging Science Experiment (HiRISE) on NASA's Mars Reconnaissance Orbiter (MRO) have narrow fields of view (McEwen et al., 2007). Their coverage of the surface is generally limited as compared to wider field instruments such as the context camera (CTX) on MRO (Malin et al., 2007).

As discussed above, blast zones around fresh craters can be observed more easily than the craters themselves, using medium-resolution (larger field of view/month-to-year cadence) instruments such as the Moderate Resolution Imaging Camera (MoRIC) on CNSA's Tianwen-1 (Yu et al., 2020), the Color and Stereo Surface Imaging Subsystem (CaSSIS) on the Trace Gas Orbiter (TGO, Thomas et al., 2017), or CTX on MRO. The latter of these has identified the majority of date-constrained impacts (Daubar et al., 2022).

We also explored the possibility that transient atmospheric phenomena (e.g., dust clouds) may have formed following an impact event of this size. Modeling on this topic conducted to date is extremely limited and mostly confined to terrestrial rather than planetary settings (Toon et al., 1982), but we nonetheless examine high-cadence (hours-to-days), wide field of view images such as those from the ESA Mars Express Visual Monitoring Camera (VMC) (Ormston et al., 2011) instrument as part of a search for these.

2.5. Instruments Involved

Table 1 lists the instruments involved in our search. Of the eight spacecraft in operation around Mars during 2022, all were involved in this effort. The pixel scale of the imagers ranges from 0.25 m (HiRISE) to ~170 km (IUVS). We group them into three categories:

- High-resolution imagers (≤1 m/pixel), providing images of small fractions of the total surface area which are selected for particular interest
- Medium-resolution imagers (1–100 m/pixel), providing images of substantial fractions of the search area; in some regions with "before" images (taken up to several years before S1222a with the same instrument) available as well as new "after" images
- Low-resolution imagers (≥100 m/pixel), providing images of the entire search area on a regular (hours-to-day cadence) basis

Table 1
The 12 Imaging Systems Involved in the Search for Any Crater Associated With the S1222a Marsquake

Spacecraft	Operator	Instrument	Pixel scale (m/px)	Type	Reference
Emirates Mars Mission, Hope (EMM)	UAESA	EXI	2,000	UV/Visible (color)	Jones et al. (2021)
ExoMars Trace Gas Orbiter (TGO)	ESA	CaSSIS	4.6	Visible (color)	Thomas et al. (2017)
Mangalyaan Mars Orbiter Mission (MOM)	ISRO	MCC	~15	Visible (color)	Arya et al. (2015)
Mars Express (MEX)	ESA	VMC	~34,000	Visible (color)	Ormston et al. (2011)
Mars Express (MEX)	ESA	HRSC	15	Visible (color)	Jaumann et al. (2007)
Mars Odyssey (M01)	NASA	THEMIS	NIR: 100/Vis: 18	NIR/Visible (color)	Christensen et al. (2004)
Mars Reconnaissance Orbiter (MRO)	NASA	HiRISE	0.25	Visible (color)	McEwen et al. (2007)
Mars Reconnaissance Orbiter (MRO)	NASA	CTX	6	Visible (greyscale)	Malin et al. (2007)
Mars Reconnaissance Orbiter (MRO)	NASA	MARCI	1,000	Visible (color)	Bell et al. (2009)
MAVEN (MAVEN)	NASA	IUVS	170,000	UV	Jakosky et al. (2015)
Tianwen-1 (TIANWEN)	CNSA	HiRIC	0.5	Visible (color)	Meng et al. (2021)
Tianwen-1 (TIANWEN)	CNSA	MoRIC	98	Visible (color)	Yu et al. (2020)

Note. Minimum possible instrument pixel scales are also included—note that all images used in this study may not be at exactly this scale. Data for MOM's MCC (spacecraft no longer operational) and Tianwen's HiRIC were examined, but did not contain any images of the region of interest after the date of S1222a. MAVEN's IUVS instrument (Jakosky et al., 2015) was imaging the surface of Mars at the time of S1222a, but not in the correct location (and in any case, nothing of relevance to this paper was seen).

2.6. Imaging Strategy

Following the occurrence of S1222a on 4 May 2022, new "before" images of the area to enable change detection could clearly not be gathered ex post facto. The low-resolution instruments' regular observations of much of Mars' surface on a daily basis meant that no novel data collection strategy was required for them. However, for some of the medium- and high-resolution instruments, specific imaging strategies could be implemented to optimize the likelihood of finding a fresh crater. The strategy devised was as follows:

- High-resolution instruments: sampling near the estimated epicenter and nearby areas of specific varied topography, to catch any "hidden" fresh blast zones immersed in shadow or on steep slopes.
- Medium-resolution instruments: Overlapping imaging of the center of the uncertainty "ellipse," working outward, with the aim of identifying new blast zones.
- Low-resolution instruments: continued regular imaging of the surface and atmosphere, with the aim of identifying new large dark spots in the days after the event, or transient atmospheric phenomena in the hours after it.

3. Results

3.1. Low-Resolution Images (≥10 m/Pixel)

Overflights of the epicentral region in the hours to days after S1222a by the VMC (and later the EXI instrument) gave no indication of new dark patches (blast zones) or unusual atmospheric phenomena.

MARCI data from across the search ellipse and farther afield using bearings from Charalambous et al. (2022) and Kim et al. (2023), gathered in the days after S1222a, also show nothing unusual when compared to images taken in the days before the event. An animation of these data is shown in the Supporting Information S1.

3.2. Medium-Resolution Images (1–10 m/Pixel)

Near-total coverage of the source region was achieved by multiple medium-resolution instruments (MoRIC, HRSC, and THEMIS in its near-infrared band). Some CTX data in the region of interest was also available. Footprints of these images are all shown in Figure 3.

No new or unusual features were found in the visible bands, and no thermal anomalies (e.g., those associated with a blast zone due to dust removal and/or surface darkening) were identified in the near-infrared.

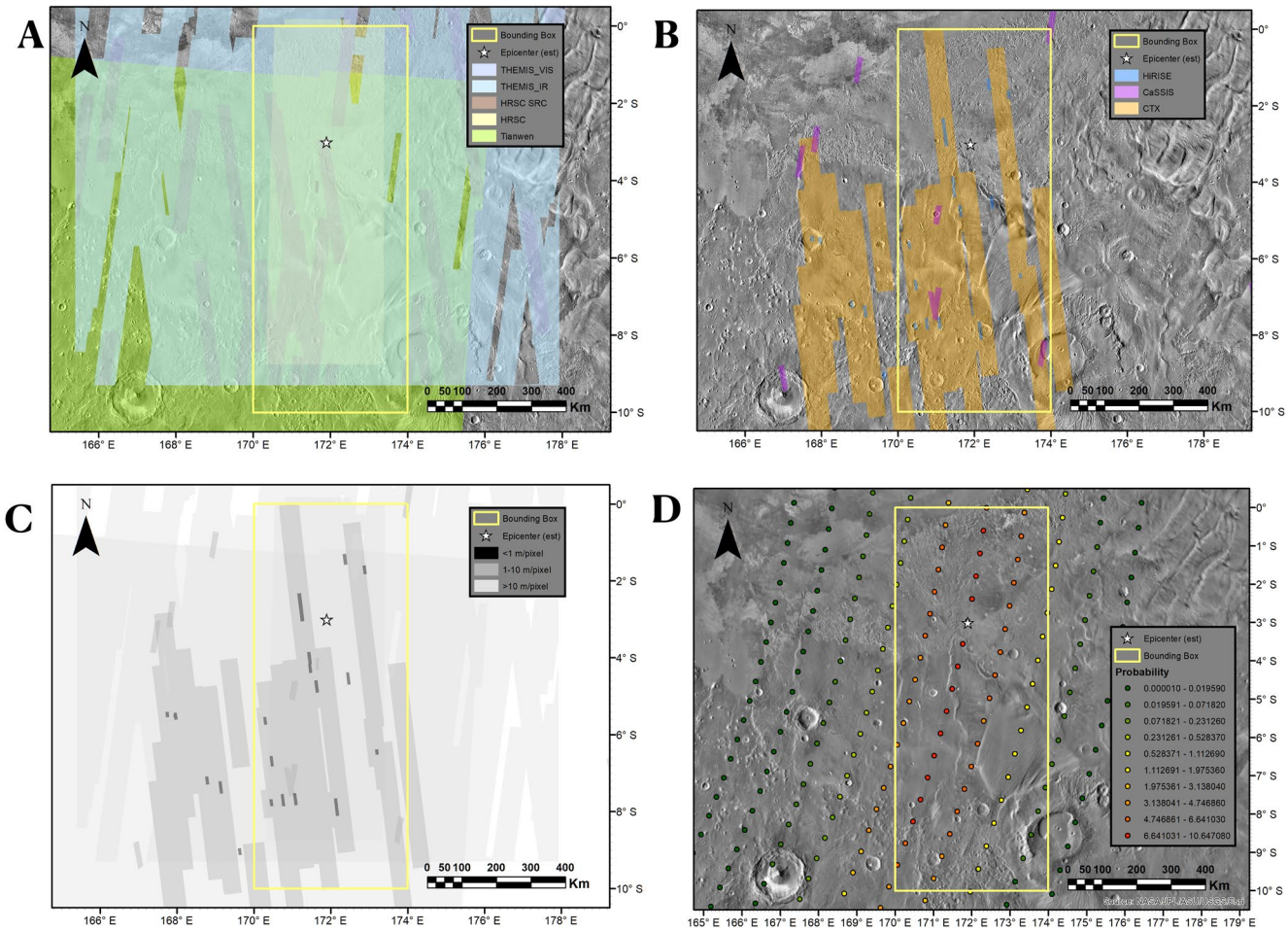

Figure 3. The areas imaged as part of this search. In all cases, the yellow rectangle shows the 10° × 4° primary search box, the white star is the body-wave estimated epicenter of S1222a, and the underlying images are from THEMIS, which mapped the entire area in visible light (~100 m/pixel). (a) and (b) Show the regional context of the imaged area, and demonstrate the near-total coverage by medium- and high-resolution instruments. For clarity, these images are split between two panels: (a) shows data from THEMIS (V/IR), HRSC (normal and stereo), and Moderate Resolution Imaging Camera (MoRIC) whilst (b) shows context camera (CTX), High-Resolution Imaging Science Experiment (HiRISE), and the Color and Stereo Surface Imaging Subsystem (CaSSIS) data. (c) Shows the variation in pixel scale with area (with ranges given to account for the fact that instrument pixel scales are not constant). (d) Shows the projections of the probability map for S1222a on area. Each dot represents the probability of the event having epicenter being in the surrounding cell. The color-coding is the probability of the event epicenter being in that cell, with red being the highest probability and green the lowest. Note that the "ellipse" formed by the probability map is irregular, accounting for the greater uncertainty in event azimuth than event distance [This figure will be a full-page landscape figure].

3.3. High-Resolution Images (≤1 m/Pixel)

A "sampling" approach was taken with high-resolution instruments, wherein a series of images across the center of the ellipse and areas of particularly steep topography were gathered. No new crater or indications of surface disturbances other than slope streaks (Lucas et al., 2023) were identified through this search, either.

The images gathered also do not support the hypothesis that the meteoroid disintegrated in the atmosphere prior to impact. The breakup of an impactor of the size required to produce the S1222a would have produced a widely-strewn spread of primary craters, of which there is no evidence in the high-resolution images. Furthermore, even if the main crater were hidden by steep topography, a large strewn field of craters would similarly be expected (Dundas et al., 2023), yet none is observed.

4. Conclusions

Multiple lines of evidence from our search of orbital images point toward S1222a not being an event of impact origin. The lines of evidence are:

The absence of a clear blast zone in low-resolution images indicates that if a crater did form, it must either be (a) smaller than can be resolved in the images, or (b) formed on unusually complex topography or on a dust-free surface, which might suppress or limit blast zone formation. Although the S1222a source region is quite dusty (Ruff & Christensen, 2002), limited areas of steep topography do exist in the surrounding area (Lucas et al., 2023).

- The absence of transient atmospheric phenomena such as dust clouds in low-resolution, global images taken immediately after S1222a (weak constraint—the formation mechanism, duration, composition, and size of any such impact-generated dust cloud on Mars are not well known)
- The absence of any new or fresh dark patches (blast zones) in any of the medium-resolution images covering the search box (strong constraint—the entire area has been mapped at medium-resolution, and given the large magnitude of this event, medium-resolution imaging should be more than sufficient to detect an impact of the expected size)
- The absence of suitable fresh craters, blast zones, or fields of secondary craters/secondary blast zones in the limited high-resolution imaging of the source region thus far (intermediate constraint—areas imaged at high-resolution are still a minority of the total search area).

These lines of reasoning lead us to conclude with a high level of confidence that the S1222a event was not associated with a meteoroid impact event. The only explanation which is consistent with current observations is a subsurface tectonic source. Future work will explore in more detail potential discriminators which this event enables, including detailed analysis of the S1222a waveforms and differences between it and large impact events from a seismic perspective.

The tectonic setting within the epicentral ellipse is very different to that of the Cerberus Fosse region where the strongest other tectonic marsquakes have occurred (Kawamura et al., 2022; Stähler et al., 2022). Initial results suggest a dip-slip fault in the mid-crust (Maguire et al., 2023), consistent with an origin between 18 and 28 km depth. Further analysis is ongoing.

Data Availability Statement

SEIS data are available from the InSight Mars SEIS Data Service at IPGP, IRIS-DMC and NASA PDS (IPGP et al., 2019).

Orbital imagery data are available online using the links given below. In each case, the URL points to a landing page. Using the instrument name, the constraining dates (4 May 2022 to 1 March 2023) and bounding boxes (0°–10°S, 170°–174°E), images and/or shapefiles can be downloaded. All images from the relevant area were downloaded and searched.

HiRISE data are available from https://www.uahirise.org/anazitisi.php, CaSSIS and HRSC data are available from the ESA Planetary Science Archive (https://archives.esac.esa.int/psa and search for "CaSSIS") VMC data are available from https://blogs.esa.int/vmc/vmc-data-archive/, CTX, MARCI, and THEMIS data are available on the NASA Planetary Data System (https://ode.rsl.wustl.edu/mars/productsearch). EXI data is available on the EMM Science Data Center Website (https://sdc.emiratesmarsmission.ae/data/exi). MoRIC data are available from the CNSA Lunar and Planetary Data Release System https://moon.bao.ac.cn/web/enmanager/mars1.

Acknowledgments
We acknowledge NASA, CNES, their partner agencies and Institutions (UKSA, SSO, DLR, JPL, IPGP-CNRS, ETHZ, IC, MPS-MPG) and the flight operations team at JPL, SISMOC, MSDS, IRIS-DMC and PDS for providing SEED SEIS data. We also express our thanks to the imager operations teams, who made special efforts to target, acquire, and search these data. CaSSIS is a project of the University of Bern and funded through the Swiss Space Office via ESA's PRODEX programme. The instrument hardware development was also supported by the Italian Space Agency (ASI) via the ASI-INAF agreement no. 2020-17-HH.0, the INAF/Astronomical Observatory of Padova, and the Space Research Center (CBK) in Warsaw. Support from SGF (Budapest), the University of Arizona (Lunar and Planetary Lab.) and NASA are also gratefully acknowledged. Operations support from Charlotte Marriner, funded by the UK Space Agency (Grants ST/R003025/1, ST/V002295/1) is also recognized. IJD was funded by NASA InSight PSP Grant 80NSSC20K0971. JL was funded by National Key R&D Program of China Grant 2022YFF0503204. GSC and NW were supported by UK Space Agency grants ST/S001514/1 and ST/T002026/1. PMG was funded by the UK Space Agency grants ST/R002355/1 and ST/V002678/1. CC was funded by the UK Space Agency under Grant ST/V00638X/1. SP and WB were supported by the InSight Project at the Jet Propulsion Laboratory, California Institute of Technology under a contract with the National Aeronautics and Space Administration (80NM0018D0004). JRH and THEMIS research were funded by the 2001 Mars Odyssey program office. DA was funded by the New York University Abu Dhabi (NYUAD) Institute Research Grant G1502 and the ASPIRE Award for Research Excellence (AARE) Grant S1560. Additionally, we are grateful to A.S. Arya of the ISRO Space Applications center for searching MOM data. As no images were acquired, no data from MOM is available to share. We also acknowledge Justin Deighan, Nick Schneider, and the MAVEN IUVS who also searched MAVEN data for images of the S1222a epicenter, of which none are available from the relevant timeframe. This manuscript constitutes InSight Contribution Number 293.

References

Arya, A., Rajasekhar, R., Singh, R., Sur, K., Chauhan, P., Sarkar, S., et al. (2015). Mars color camera onboard Mars orbiter mission: Initial observations and results. In *46th annual Lunar and planetary science conference* (p. 2123).

Banerdt, W. B., Smrekar, S. E., Banfield, D., Giardini, D., Golombek, M., Johnson, C. L., et al. (2020). Initial results from the insight mission on Mars. *Nature Geoscience*, *13*(3), 183–189. https://doi.org/10.1038/s41561-020-0544-y

Bart, G. D., Daubar, I. J., Ivanov, B. A., Dundas, C. M., & McEwen, A. S. (2019). Dark halos produced by current impact cratering on Mars. *Icarus*, *328*, 45–57. https://doi.org/10.1016/j.icarus.2019.03.004

Bell, J. F. I., Wolff, M. J., Malin, M. C., Calvin, W. M., Cantor, B. A., Caplinger, M. A., et al. (2009). Mars reconnaissance orbiter Mars color imager (MARCI): Instrument description, calibration, and performance. *Journal of Geophysical Research*, *114*(E8). https://doi.org/10.1029/2008JE003315

Ceylan, S., Clinton, J. F., Giardini, D., Böse, M., Charalambous, C., Van Driel, M., et al. (2021). Companion guide to the marsquake catalog from insight, sols 0–478: Data content and non-seismic events. *Physics of the Earth and Planetary Interiors*, *310*, 106597. https://doi.org/10.1016/j.pepi.2020.106597

Ceylan, S., Clinton, J. F., Giardini, D., Stähler, S. C., Horleston, A., Kawamura, T., et al. (2022). The marsquake catalogue from insight, sols 0–1011. *Physics of the Earth and Planetary Interiors*, *333*, 106943. https://doi.org/10.1016/j.pepi.2022.106943

Charalambous, C., Pike, T., Fernando, B., Stott, A., Nissen-Meyer, T., & Lognonné, P. (2022). Denoising insight: Determination of Mars' lateral crustal variations through surface-wave identification (Tech. Rep.). EPSC Abstracts, 2022.

Charalambous, C., Stott, A. E., Pike, W., McClean, J. B., Warren, T., Spiga, A., et al. (2021). A comodulation analysis of atmospheric energy injection into the ground motion at insight, Mars. *Journal of Geophysical Research: Planets*, *126*(4), e2020JE006538. https://doi.org/10.1029/2020je006538

Christensen, P. R., Jakosky, B. M., Kieffer, H. H., Malin, M. C., McSween, H. Y., Nealson, K., et al., (2004). The thermal emission imaging system (THEMIS) for the Mars 2001 odyssey mission. *Space Science Reviews*, *110*(1/2), 85–130. https://doi.org/10.1023/b:spac.0000021008.16305.94

Daubar, I. J., Dundas, C. M., Byrne, S., Geissler, P., Bart, G., McEwen, A. S., et al. (2016). Changes in blast zone albedo patterns around new Martian impact craters. *Icarus*, *267*, 86–105. https://doi.org/10.1016/j.icarus.2015.11.032

Daubar, I. J., Dundas, C. M., McEwen, A. S., Gao, A., Wexler, D., Piqueux, S., et al. (2022). New craters on Mars: An updated catalog. *Journal of Geophysical Research: Planets*, *127*(7), e2021JE007145. https://doi.org/10.1029/2021je007145

Daubar, I. J., Fernando, B. A., Garcia, R. F., Grindrod, P. M., Zenhäusern, G., Wójcicka, N., et al. (2023). Two seismic events from insight confirmed as new impacts on Mars. *The Planetary Science Journal*, *4*(9), 175. https://doi.org/10.31223/X5894H

Daubar, I. J., McEwen, A., Byrne, S., Kennedy, M., & Ivanov, B. (2013). The current Martian cratering rate. *Icarus*, *225*(1), 506–516. https://doi.org/10.1016/j.icarus.2013.04.009

Dundas, C. M., Mellon, M. T., Posiolova, L. V., Miljković, K., Collins, G. S., Tornabene, L. L., et al. (2023). A large new crater exposes the limits of water ice on Mars. *Geophysical Research Letters*, *50*(2), e2022GL100747. https://doi.org/10.1029/2022gl100747

Garcia, R. F., Daubar, I. J., Beucler, E., Posiolova, L. V., Collins, G. S., Lognonné, P., et al. (2022). Newly formed craters on Mars located using seismic and acoustic wave data from insight. *Nature Geoscience*, *15*(10), 774–780. (Citation Key: Garcia2022). https://doi.org/10.1038/s41561-022-01014-0

Hartmann, W., & Daubar, I. (2017). Martian cratering 11. Utilizing decameter scale crater populations to study Martian history. *Meteoritics & Planetary Science*, *52*(3), 493–510. https://doi.org/10.1111/maps.12807

InSight Marsquake Service. (2023). *Mars Seismic Catalogue, InSight Mission; V13 2023-01-01*. ETHZ, IPGP, JPL, ICL, Univ. Bristol. https://doi.org/10.12686/a19

IPGP, JPL, CNES, ETHZ, ICL, MPS, & MFSC (2019). Insight Mars SEIS data service. https://doi.org/10.18715/SEIS.INSIGHT.XB_2016

Jakosky, B. M., Lin, R. P., Grebowsky, J. M., Luhmann, J. G., Mitchell, D., Beutelschies, G., et al. (2015). The Mars atmosphere and volatile evolution (MAVEN) mission. *Space Science Reviews*, *195*(1–4), 3–48. https://doi.org/10.1007/s11214-015-0139-x

Jaumann, R., Neukum, G., Behnke, T., Duxbury, T. C., Eichentopf, K., Flohrer, J., et al. (2007). The high-resolution stereo camera (HRSC) experiment on Mars express: Instrument aspects and experiment conduct from interplanetary cruise through the nominal mission. *Planetary and Space Science*, *55*(7–8), 928–952. https://doi.org/10.1016/j.pss.2006.12.003

Jones, A., Wolff, M., Alshamsi, M., Osterloo, M., Bay, P., Brennan, N., et al. (2021). The emirates exploration imager (EXI) instrument on the emirates Mars mission (EMM) hope mission. *Space Science Reviews*, *217*(8), 1–56. https://doi.org/10.1007/s11214-021-00852-5

Kawamura, T., Clinton, J. F., Zenhäusern, G., Ceylan, S., Horleston, A. C., Dahmen, N. L., et al. (2022). S1222a - The largest marsquake detected by insight. *Geophysical Research Letters*, *n/a*(n/a), e2022GL101543. https://doi.org/10.1029/2022GL101543

Kim, D., Banerdt, W. B., Ceylan, S., Giardini, D., Lekić, V., Lognonné, P., et al. (2022). Surface waves and crustal structure on Mars. *Science*, *378*(6618), 417–421. https://doi.org/10.1126/science.abq7157

Kim, D., Stähler, S. C., Ceylan, S., Lekic, V., Maguire, R., Zenhäusern, G., et al. (2023). Structure along the Martian dichotomy constrained by Rayleigh and love waves and their overtones. *Geophysical Research Letters*, *50*(8), e2022GL101666. https://doi.org/10.1029/2022gl101666

Lognonné, P., Banerdt, W. B., Giardini, D., Pike, W. T., Christensen, U., Laudet, P., et al. (2019). SEIS: Insight's seismic experiment for internal structure of Mars. *Space Science Reviews*, *215*, 1–170. https://doi.org/10.1007/s11214-018-0574-6

Lucas, A., Daubar, I. J., Le Teuff, M., Posiolova, L. V., Sainton, G., Mangeney, A., et al. (2023). Discussion on seismically triggered avalanches on Mars. *Authorea Preprints*. https://doi.org/10.22541/essoar.167839703.36993709/v1

Maguire, R., Lekic, V., Kim, D., Schmerr, N. C., Li, J., Beghein, C., et al. (2023). Moment tensor estimation of event s1222a and implications for tectonics near the dichotomy boundary in southern Elysium Planitia, Mars. Preprint submitted to ESSOAr.

Malin, M. C., Bell, J. F., Cantor, B. A., Caplinger, A. M., Calvin, W. M., Clancy, R. T., et al. (2007). Context camera investigation on board the Mars reconnaissance orbiter. *Journal of Geophysical Research*, *112*(E5), E05S04. https://doi.org/10.1029/2006JE002808

McEwen, A. S., Eliason, E. M., Bergstrom, J. W., Bridges, N. T., Hansen, C. J., Delamere, W. A., et al. (2007). Mars reconnaissance orbiter's high resolution imaging science experiment (HIRISE). *Journal of Geophysical Research*, *112*(E5), E05S02. https://doi.org/10.1029/2005je002605

Meng, Q., Wang, D., Wang, X., Li, W., Yang, X., Yan, D., et al. (2021). High resolution imaging camera (HIRIC) on China's first Mars exploration Tianwen-1 mission. *Space Science Reviews*, *217*(3), 1–29. https://doi.org/10.1007/s11214-021-00823-w

Ormston, T., Denis, M., Scuka, D., & Griebel, H. (2011). An ordinary camera in an extraordinary location: Outreach with the Mars Webcam. *Acta Astronautica*, *69*(7–8), 703–713. https://doi.org/10.1016/j.actaastro.2011.04.015

Posiolova, L. V., Lognonné, P., Banerdt, W. B., Clinton, J., Collins, G. S., Kawamura, T., et al. (2022). Largest recent impact craters on Mars: Orbital imaging and surface seismic co-investigation. *Science*, *378*(6618), 412–417. https://doi.org/10.1126/science.abq7704

Ruff, S. W., & Christensen, P. R. (2002). Bright and dark regions on Mars: Particle size and mineralogical characteristics based on thermal emission spectrometer data. *Journal of Geophysical Research*, *107*(E12), 2-1. https://doi.org/10.1029/2001je001580

Stähler, S. C., Mittelholz, A., Perrin, C., Kawamura, T., Kim, D., Knapmeyer, M., et al. (2022). Tectonics of Cerberus Fossae unveiled by marsquakes. *Nature Astronomy*, *6*(12), 1376–1386. https://doi.org/10.1038/s41550-022-01803-y

Taylor, S. R., Velasco, A. A., Hartse, H. E., Phillips, W. S., Walter, W. R., & Rodgers, A. J. (2002). Amplitude corrections for regional seismic discriminants. In *Monitoring the comprehensive Nuclear-Test-Ban Treaty: Seismic event discrimination and identification*. (pp. 623–650).

Thomas, N., Cremonese, G., Ziethe, R., Gerber, M., Brändli, M., Bruno, G., et al. (2017). The colour and stereo surface imaging system (CASSIS) for the exomars trace gas orbiter. *Space Science Reviews*, *212*(3–4), 1897–1944. https://doi.org/10.1007/s11214-017-0421-1

Toon, O. B., Pollack, J. B., Ackerman, T. P., Turco, R. P., McKay, C. P., & Liu, M. (1982). Evolution of an impact-generated dust cloud and its effects on the atmosphere. In *Geological implications of impacts of large asteroids and comets on the Earth*.

Walter, W. R., Dodge, D. A., Ichinose, G., Myers, S. C., Pasyanos, M. E., & Ford, S. R. (2018). Body-wave methods of distinguishing between explosions, collapses, and earthquakes: Application to recent events in North Korea. *Seismological Research Letters*, *89*(6), 2131–2138. https://doi.org/10.1785/0220180128

Wojcicka, N., Collins, G. S., Bastow, I. D., Teanby, N. A., Miljković, K., Rajšić, A., et al. (2020). The seismic moment and seismic efficiency of small impacts on Mars. *Journal of Geophysical Research: Planets*, *125*(10), e2020JE006540. https://doi.org/10.1029/2020je006540

Wójcicka, N., Zenhäusern, G., Collins, G. S., Stähler, S. C., Daubar, I. J., Knapmeyer, M., et al. (2023). Impact rate on Mars implied by seismic observations. In *54th Lunar and planetary science conference 2023 (LPI contrib. no. 2806)*.

Yu, G., Liu, E., Liu, G., Zhou, L., Zeng, J., Chen, Y., et al. (2020). Moderate resolution imaging camera (MORIC) of China's first Mars mission Tianwen-1. *Earth and Planetary Physics*, *4*(4), 364–370.